Effect of the synergistic anion on electron paramagnetic resonance spectra of iron–transferrin anion complexes is consistent with bidentate binding of the anion

Jean Dubach,* Betty Jean Gaffney,‡ Kundalika More,* Gareth R. Eaton,* and Sandra S. Eaton*
*Departments of Chemistry, University of Denver, Denver, Colorado 80208; and ‡The Johns Hopkins Unversity, Baltimore, Maryland 21218 USA

ABSTRACT Continuous wave (cw) X-band EPR spectra at ~ 90 K were obtained for iron–transferrin–anion complexes with 18 anions. Each anion had a carboxylate group and at least one other polar moiety. As the second polar group was varied from hydroxyl to carbonyl to amine to carboxylate, the EPR spectra changed from a dominant signal at g' ~ 4.3 with a second smaller peak at g' ~ 9 to a broad signal with intensity between g' ~ 5 and 7. Computer simulation indicated that the changes in the EPR spectra were due to changes in the zero field splitting parameter ratio, E/D, from ~⅓ for carbonate anion to ~0.04 for malonate anion. Observation of iron–^{13}C coupling in the electron spin echo envelope modulation (ESEEM) for iron transferrin [1-^{13}C]pyruvate indicated that the carboxylate group was bound to the iron. It is proposed that all of the anions behave as bidentate ligands, with coordination to the iron through both the carboxylate and proximal groups, and the carboxyl group serves as a bridge between the iron and a positively charged group on the protein.

INTRODUCTION

Human serum transferrin is a member of a class of iron-binding proteins, designated as siderophilins, that is widely distributed through the animal kingdom (1). A synergistic anion is required for metal binding, and there are two metal-synergistic anion binding sites per protein (1,2). The naturally occurring synergistic anion is carbonate. Nonsynergistic anions (chloride, perchlorate, et cetera) also bind to transferrin to alter the iron-binding site indirectly through conformational changes in the protein (3). There is considerable interest in understanding the interaction of both synergistic and nonsynergistic anions with the metal and the protein because it has been suggested that both types of anion play a role in the removal of iron from transferrin in vivo (4). This paper examines the mode of synergistic anion binding. Preliminary reports of this work were presented at MR-90, Brisbane, Australia; 1–5 July 1990 (Abstr. P-9) and 32nd Rocky Mountain Conference, Denver, CO, 29 July–3 August 1990 (Abstr. 308).

Schlabach and Bates (2) used visible spectroscopy to determine which anions could substitute for carbonate as the synergistic anion in the iron–transferrin complex. They concluded that a carboxylate group and a proximal polar group (hydroxy, keto, amino, or carboxylate) within 6.3 to 7.0 Å of the carboxylate were required for synergistic binding (2). At most one bulky group could be present on the carbon α to the carboxylate. They proposed a model in which the carboxylate group of the anion interacts with a positively charged group on the protein, while the proximal functional group binds to the iron.

In the EPR spectra of vanadyl–transferrin–anion complexes of anions containing a carboxylate and a proximal group, the value of a_I was found to be anion dependent (5). On this basis, it was proposed that the proximal group was coordinated to the vanadyl.

Coordination of carbonate anion to the metal bound to transferrin has been demonstrated by several spectroscopic studies. ^{13}C–metal coupling was observed in nuclear magnetic resonance (NMR) studies of ^{205}Tl (6) and ^{113}Cd (7) transferrin complexes with $^{13}CO_3^{2-}$ and in electron spin echo envelope modulation (ESEEM) studies of vanadyl (8), Cu(II) (9), and Fe (III) (9) complexes of transferrin with $^{13}CO_3^{2-}$. ESEEM studies of the Cu(II) and vanadyl complexes of Tf indicated bidentate coordination of oxalate anion (8). Inequivalence of the ^{13}C NMR signals for ^{13}C-oxalate bound to GaTf was interpreted as indicating that one end of the oxalate was bound to the metal and the other end interacted with the protein (10). An alternate interpretation of those results is that both ends of the oxalate are bound to the metal, but the two ends interact differently with the protein environment (8).

The x-ray crystal structures of $FeTfCO_3$ at 3.3 Å resolution (11) and of $FeLfCO_3$ at 3.2 Å resolution (12) showed that the protein provided four ligands to the iron (two tyrosines, one histidine, and one aspartate), leaving two sites available for interaction with anion and/or water. After completion of the work reported in this paper, a higher resolution structure of $FeLfCO_3$ showed that the carbonate was bound to the iron as a bidentate ligand (13).

0006-3495/91/05/1091/10 $2.00

Aisen et al. reported the EPR spectra for FeTfanion complexes in which the anion was carbonate, NTA, thioglycollate, malonate, and oxalate (14,15). The spectra were strongly dependent on the anion, which suggested that EPR studies of a wider range of anions might help to elucidate the mode of anion binding.

This paper reports the EPR spectra of iron transferrin anion complexes of 18 anions with a variety of proximal groups, including 15 anions for which visible spectroscopy data were reported by Schlabach and Bates (2). The EPR spectrum of $FeTfCO_3$ had been analyzed previously by computer simulation (16). To interpret the observed changes in the spectra, the distinctive spectra of FeTfoxalate and FeTfmalonate were computer simulated. To determine whether the carboxylate group of the anion was bound to the iron, ESEEM data were obtained for the iron transferrin complexes of pyruvate and [1-^{13}C]pyruvate.

METHODS

Materials

Hepes buffer and iron-free human transferrin (Tf) were obtained from Sigma Chemical Co. (St. Louis, MO) and used without further purification. Anions were obtained from standard chemical suppliers. The sodium salt of 99%-enriched [1-^{13}C]pyruvate was purchased from Isotec, Inc. Disposable plastic tubes and pipettes were used with all protein solutions, except for EPR measurements which were performed in 4-mm O.D. quartz tubes.

Preparation of complexes

Iron–transferrin–anion complexes were formed by a procedure similar to that reported by Schlabach and Bates (2) and by Najarian et al. (17). For anions other than carbonate, a nitrogen-filled glove box was used to maintain a CO_2-free atmosphere for complex formation (18,19). The apoprotein was dissolved in 0.09 M Hepes buffer at pH 3.5–4.0 and purged with nitrogen gas to remove traces of CO_2. $FeCl_3$ was added to an acidic solution of the anion and the mixture was added to the apoprotein. The Fe(III) concentration was equal to the concentration of binding sites and the anion concentration was about three times the concentration of Fe(III). The pH was adjusted to 7.5 with ammonia mixed with nitrogen gas that had been passed over a 2 N KOH trap to remove CO_2. Samples for EPR spectra were mixed with an equal volume of glycerol and frozen immediately in liquid nitrogen. The protein concentration in the final solution was 0.5 to 1.0 mM.

To examine the effects of salt on the EPR spectra of FeTfoxalate, 80 mg Tf was dissolved in 1 ml of nitrogen-saturated buffer containing 0.090 M Hepes, 35 mM oxalic acid, and enough ammonium hydroxide to adjust the pH to 7.5. This solution was placed in a dialysis bag in 0.25 liter of the same buffer. With nitrogen bubbling through the dialysis buffer, solid $FeSO_4$ was added to the external solution to bring the concentration to 2 mM in Fe(II). After 4 h, the dialysis bag containing the red FeTf oxalate solution was transferred to 1 liter of iron-free dialysis buffer and dialysis was continued for 24 h with one change of buffer. EPR spectra were recorded for the resulting FeTfoxalate solution and for solutions to which volumes of 2 M NaCl were added to bring the NaCl concentration in the final solution to 0.5 and 1.0 M.

Carbonate displacement with oxalate

A sample of $FeTfCO_3$ in which the metal-anion binding sites were fully saturated was prepared by allowing the sample to stand overnight in the presence of excess sodium bicarbonate at room temperature. The solution was then flushed with nitrogen gas to remove excess carbonate. A solution containing excess sodium oxalate was added and the solution was allowed to stand overnight in a nitrogen atmosphere at room temperature. The extent of carbonate displacement was estimated by comparing the amplitude of the $FeTfCO_3$ (1,560 G) and FeTfoxalate (1,230 G) peaks in the EPR spectra with the amplitudes observed for the complexes at known concentrations. A 35-fold excess of oxalate was sufficient to convert essentially all of the protein to FeTfoxalate.

Visible spectra

A Cary-14 spectrophotometer with the On-Line Instruments OLIS 3920Z modification was used to record visible spectra of samples in a 0.5-ml quartz cuvette with an airtight cap and a 1.0-cm light path.

EPR spectra

Cw X-band EPR spectra were recorded at ~ 90 K on an IBM ER200 or Varian E9 spectrometer with 100 kHz modulation at modulation amplitudes and microwave powers that did not cause line shape distortion. Cw EPR spectra of some of the samples also were obtained at 5–7 K with an Oxford ESR900 cryostat on the same spectrometers. The spectra at 5–7 K were slightly sharper than at 90 K, but the characteristic dependence on anion was unchanged.

Pulsed EPR data were obtained with two- and three-pulse sequences on a spectrometer that has been described previously (20). Two-pulse data consisted of 1,024 data points at 2-ns intervals starting at 220 ns. Three-pulse data consisted of 1,700 data points at 6-ns intervals starting at 330 ns. Temperature was controlled at 2–3 K with an Oxford ESR910 pumped liquid helium cryostat. The magnetic field was set to the $g' = 4.3$ signal. The ESEEM data were cosine Fourier transformed to determine the characteristic modulation frequencies. The method of Mims (21) was used to extrapolate the data into the instrument "dead time." The analysis of the ^{13}C modulation frequencies to obtain the value of the iron–^{13}C coupling constant was performed as reported for the analysis of the ESEEM data for $FeTf[^{13}CO_3]$ (9).

Characterization of complexes

The visible spectra of the FeTfanion complexes had bands between 400 and 480 nm and were in good agreement with literature spectra (2). Most of the complexes were reddish, but the phenyllactate and lactate complexes were yellow. The positions of the bands in the visible spectra did not correlate with the dependence of the EPR spectra on anion. Thus, the EPR spectra provide information on a different aspect of the metal binding environment than the visible spectra do.

The EPR spectra of the FeTf complexes with carbonate, NTA, oxalate, and malonate agreed with those reported by Aisen et al. (14,15).

For each of the anions, EPR spectra were recorded for solutions of Fe(III) and anion in buffer-glycerol, without Tf. Under the experimental conditions that were used to record the spectra of FeTfanion, most of these solutions did not give an observable EPR signal between $g' = 4$ and 8. For the NTA, oxalate, maleate, and pyruvate anions, there was an EPR signal near $g' = 4.3$, but the g' values and lineshapes were distinctly different from those for the spectrum of the corresponding FeTfanion complex. These differences demonstrated that the signal

observed in the presence of Tf was due to FeTfanion and not an Fe(anion) complex. Although an earlier report (5) listed glycine as a nonsynergistic anion, the spectra of FeTf glycine differed from those of Fe(III) glycine without Tf, indicating that glycine should be reclassified as a synergistic anion. For three other anions (citrate, succinate, and EDTA) the EPR spectra of the mixture of Fe(III) and anion was the same as for the mixture of Fe(III), anion, and transferrin. For these anions the characteristic band was also absent from the visible spectra of solutions containing Fe, Tf, and anion, so it was concluded that an FeTfanion complex was not formed.

RESULTS AND DISCUSSION

FeTfanion complex formation with the 18 anions studied was indicated by the characteristic charge-transfer visible spectra. Most of the anions are in three groups as shown in chart 1: I, carboxylate with a proximal polar group (OH, keto, or amino); II, dicarboxylate plus additional polar group, and III, dicarboxylate or carboxamide. Carbonate and NTA are special cases. Spectra of complexes with carbonate, NTA, and anions in group I had a strong peak in the EPR spectrum at 1,570 G ($g' \sim 4.3$) and a weaker signal at 750 G ($g' \sim 9$) (Fig. 1). As the proximal group was varied from OH to keto to amino, the low-field signals broadened and shifted upfield and a shoulder at 1,300 G ($g' \sim 5.2$) became

Chart 1

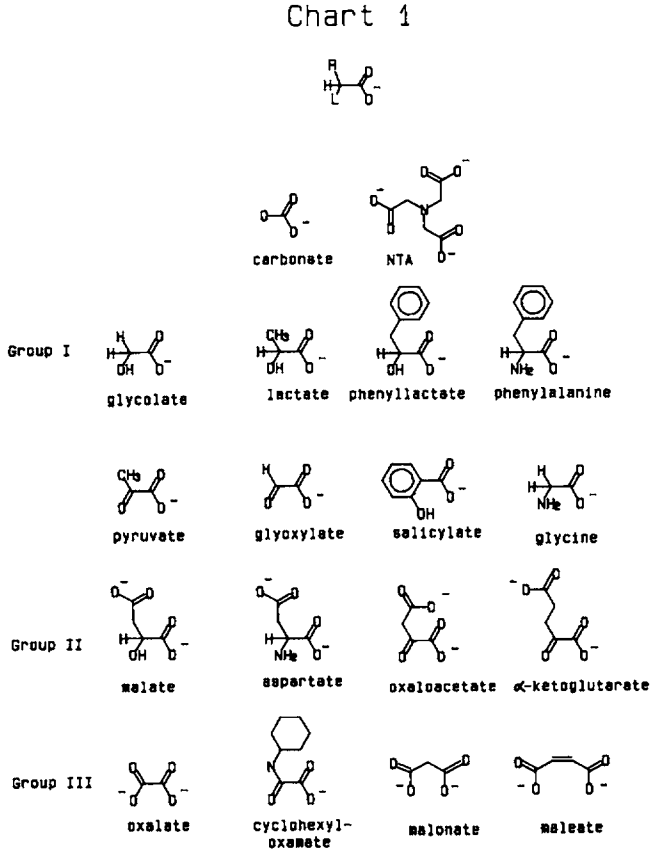

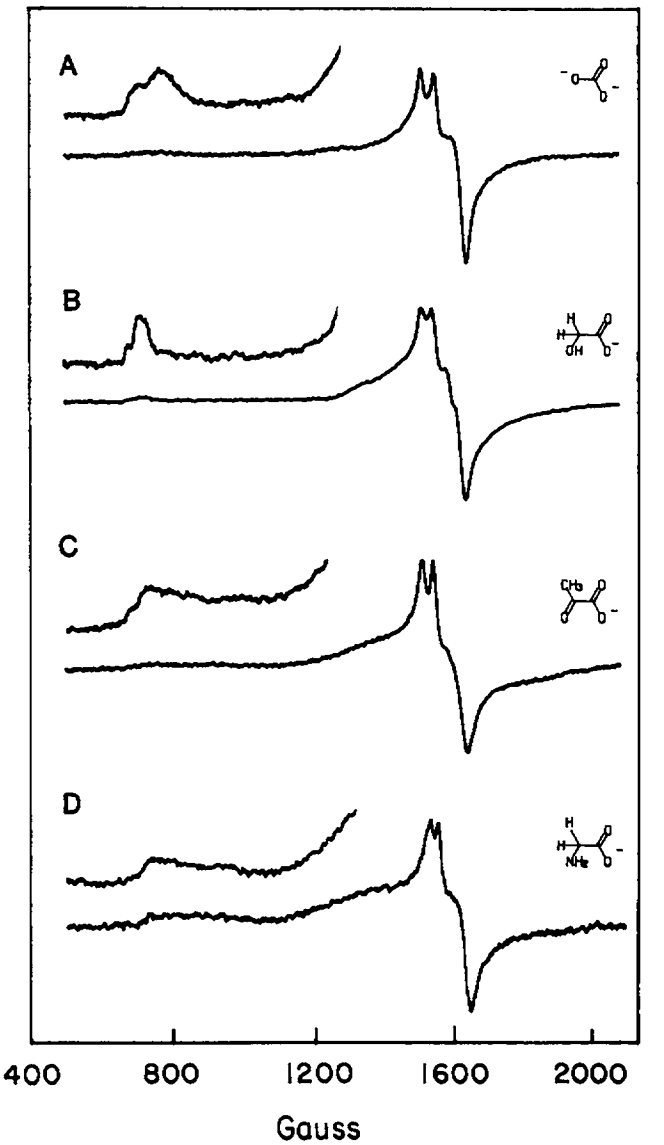

FIGURE 1 X-band EPR spectra for FeTfanion complexes in water: glycerol solutions containing 0.045 M Hepes. The anion was (*A*) carbonate, (*B*) glycolate, (*C*) pyruvate, and (*D*) glycine. Spectra were recorded at ~90 K with the following instrument settings: time constant, 0.33 s; scan time, 4 min.; modulation amplitude, 5–10 G; microwave power, 20 mW; and microwave frequency, 9.45 GHz.

more prominent (Fig. 1). The dependence of the EPR spectra on the proximal group is consistent with previous proposals that this group binds to the iron (2,6). In the spectra of the complexes with anions in group III all of the signal intensity was between ~ 950 and 1,300 G ($g' \sim 7$ to 5.2) (Fig. 2). The spectra of the complexes with the anions in group II had peaks at ~ 770 and 1,570 G as well as substantial signal intensity between 950 and 1,300 G (Fig. 3, *a* and *b*). It is proposed that these

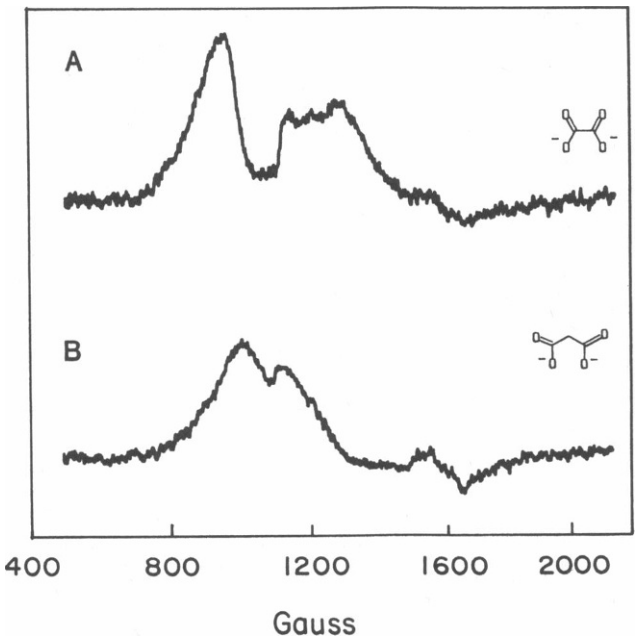

FIGURE 2 X-band EPR spectra for (*A*) FeTfoxalate and (*B*) FeTfmalonate in water:glycerol solution containing 0.045 M Hepes. Spectra were recorded at ~ 90 K with instrument settings: time constant, 0.33 s; scan time, 4 min; modulation amplitude, 10 G; microwave power, 20 mW; and microwave frequency, 9.45 GHz.

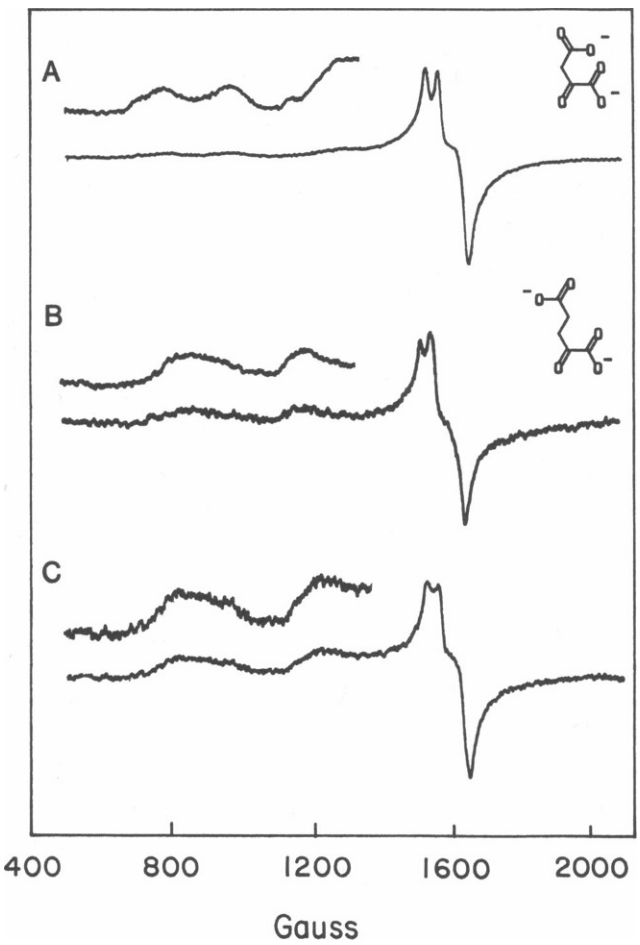

FIGURE 3 X-band EPR spectra of FeTfanion complexes in water: glycerol solutions containing 0.045 M Hepes: (*A*) FeTfoxaloacetate, (*B*) FeTfα-ketoglutarate, (*C*) approximately equimolar mixture of FeTfcarbonate and FeTfoxalate. Spectra were recorded at ~ 90 K with instrument settings: time constant, 0.33 s; scan time, 4 min; modulation amplitude, 10 G; microwave power, 20 mW; and microwave frequency, 9.45 GHz.

spectra are combinations of the spectra observed for the anions in groups I and III. This assignment is supported by the spectrum in Fig. 3 *c*, which was obtained for a sample of $FeTfCO_3$ to which a fivefold excess of oxalate had been added to displace some of the carbonate. The sample contained approximately equal amounts of $FeTfCO_3$ and FeTfoxalate. The EPR spectrum of the mixture is similar to that observed for the complexes with anions in group II (Fig. 3, *a* and *b*), which indicates that the anions in group II bind in the manner either of the dicarboxylates or of the carboxylates with a second polar group, with approximately equal probability.

Assignment of the EPR spectra of FeTfoxalate and FeTfmalonate

Lineshapes for the EPR spectra of the native, carbonate complex of FeTf were simulated previously (16). For this complex the spectrum is dominated by a signal at $g' \sim 4.3$ (~1,600 G at X-band). The $g' \sim 4.3$ signal arises from transitions between the energy levels of the middle Kramers doublet of the $S = \frac{5}{2}$ high spin Fe(III). It is of high amplitude primarily because the anisotropy is small. For $E/D \sim \frac{1}{3}$, spectral intensity from transitions in the lower doublet is more than an order of magnitude lower than for the middle doublet due to large anisotropy in the lower doublet.

A quite different situation arises when E/D is near zero, for which high-spin Fe(III) porphyrins, including methemoglobin azide, are examples. For $E/D \sim 0$, the spectral amplitude is dominated by overlapping g_x and g_y features at $g' \sim 6.0$ for the lower Kramer's doublet, but with intensity spread to $g_z = 2.0$ in a typical powder pattern for axial symmetry. For $E/D = 0$, the value of g_z for the middle Kramers doublet is also = 6.0, but it does not contribute to the observed spectrum because the transition probability is zero. Even though the transition probabilities for the transitions in the middle doublet for $E/D = 0$ become nonzero near the x and y principal axis directions, the anisotropy of transitions in this doublet is

so large, extending from $g' = 6.0$ to < 1.0, that there is no significant contribution to the observed spectrum. Signal intensity from transitions in the upper Kramers doublet, for all values of E/D, is negligible, unless D is several times smaller than the microwave quantum, because anisotropy is very large and transition probabilities are small.

The EPR spectrum of FeTfoxalate was reported previously (14,15), but was not analyzed. The distinctive spectra of FeTfoxalate and FeTfmalonate are intermediate between the extremes discussed above. The ratio E/D is between the limiting values of 0 and ⅓, and the spectral intensity in the region above $g' = 2.0$ arises from significant contributions from transitions between levels of both the low and middle Kramers doublets. Fig. 4 illustrates this point by showing simulated spectra for the low-field region for E/D between 0.1 and 0.2. The model used for the simulations shown in Fig. 4 is the same one that was used by Yang and Gaffney in simulations of the spectra of $FeTfCO_3$ (16). The model attributes the dominant source of line-broadening to a Gaussian distribution in values of E/D. Other important input variables in the simulations are the spin-packet line width and the energy level separation, D. The value of D for $FeTfCO_3$, 0.25 cm^{-1}, is unusually small for low-symmetry Fe(III) complexes and is smaller than the X-band microwave quantum (22). This value of D was used in the simulations shown in Fig. 4. When D is less than the microwave quantum, the g'-value for the low-field component of a spectrum (from the lower Kramers doublet) can be simulated with several combinations of E/D and D. However, the g'-values and relative heights of the combined features resulting from both the low- and mid-doublet transitions are quite diagnostic for values of D smaller than the microwave quantum. Another consequence of the small value of D is that all three Kramers doublets are equally populated down to temperatures < 4 K.

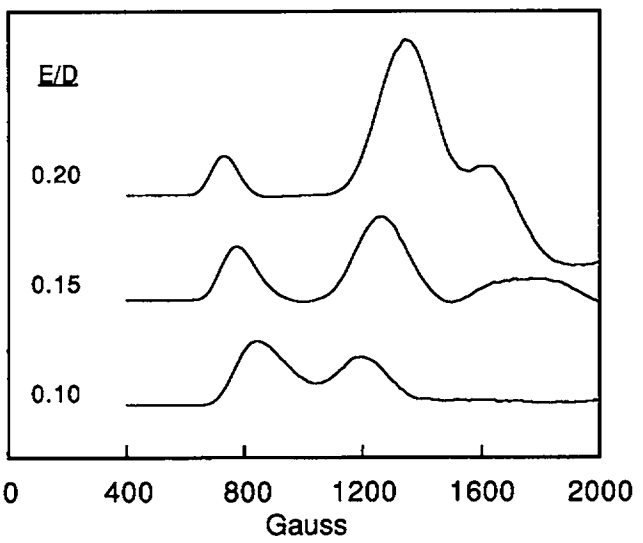

FIGURE 4 The hypothetical simulated EPR spectra shown are the sum of calculated transitions between levels of the lower and middle Kramers doublets of a spin 5/2 system. Values of the zero-field splitting parameters were 0.25 cm^{-1} for D and 0.1 to 0.2 for the ratio E/D. The maximum at low field is the g_y feature from the lower doublet spectrum; the higher field maximum is the g_x feature of the middle doublet spectrum. The figure results from a Gaussian distribution of E/D values with a half-width of 0.04 and a field-swept Lorentzian (FSL) line width of 500 MHz (the apparent line width in the field-swept spectra is therefore proportional to 500 MHz/g').

Chloride is a nonsynergistic anion that is known to affect the details of iron transferrin EPR spectra (3) and is an important parameter in release of iron from the protein (4). Experiments with NH_2-terminal and COOH-terminal monoferric transferrins showed that each iron site exhibits two EPR spectra and chloride alters the conformational equilibria between the states that give rise to these EPR spectra (3). To obtain experimental information about parameters in the spectral simulation, NaCl was added to solutions of FeTfoxalate (16). Fig. 5 shows experimental spectra for 0, 0.5, and 1.0-M NaCl solutions. (The difference between the spectra in Figs. 2 A and 5 A shows the effect of glycerol on the EPR spectra.) The changes in the spectra in Fig. 5 as a function of NaCl concentration are consistent with changes in the relative amounts of two species of coordinated iron. A change in relative populations of two species as a function of NaCl concentration was also seen for $FeTfCO_3$ (3,16). The values of E/D that provided the best set of simulated spectra for FeTfoxalate as a function of NaCl concentration are 0.06 and 0.10. The fit was optimized with different linewidths and different E/D distribution widths for the two species. Fig. 6 shows the effects of combining the spectra from the two species in different proportions. Simulated spectra *b* and *d* in Fig. 6 gave the best match to the experimental spectra of FeTfoxalate in 0 and 1.0 M NaCl, respectively. Fig. 7 shows an overlay of the experimental and simulated spectra. No attempt was made to add a third signal for the small amount of $FeTfCO_3$ signal at $g' = 4.3$ (indicated by the arrow in the figure). Fig. 8 shows a simulation for FeTfmalonate. In this case, only one species was used in the simulation because the spectral features overlap so extensively that a more detailed analysis was not warranted. It is clear, however, that most of the intensity in the spectrum of FeTfmalonate can be accounted for by a distribution in E/D and contributions from both Kramers doublets. In Table 1 values of parameters used in these spectral simulations

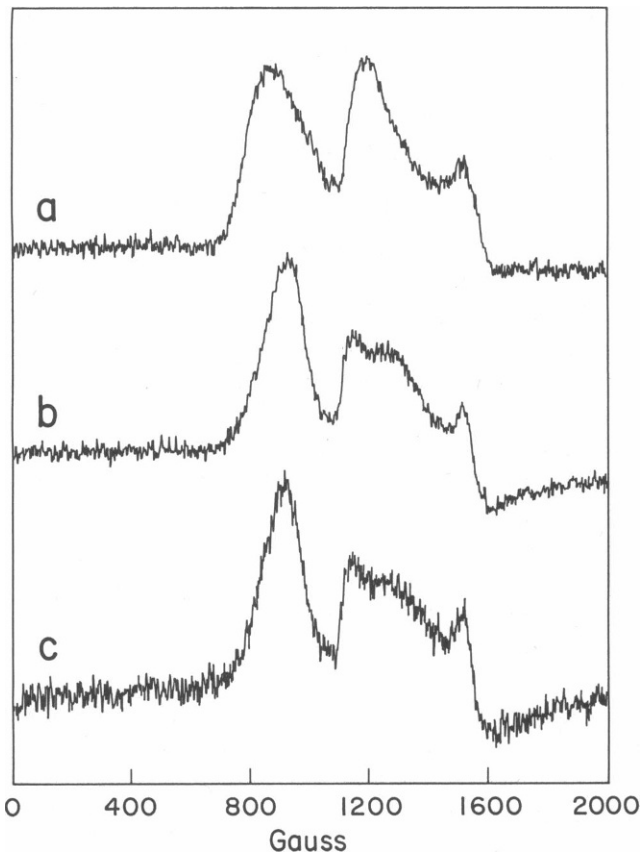

FIGURE 5 Experimental EPR spectra for FeTfoxalate in buffers containing (*a*) 0, (*b*) 0.5, and (*c*) 1.0 M NaCl. The concentrations of FeTfoxalate were (*a*) 1.0, (*b*) 0.75, and (*c*) 0.50 mM. Spectra were recorded at 80 K with instrument settings: time constant, 0.128 s; scan time, 8 min; modulation amplitude, 10 G; microwave power, 1 mW; and microwave frequency, 9.21 GHz.

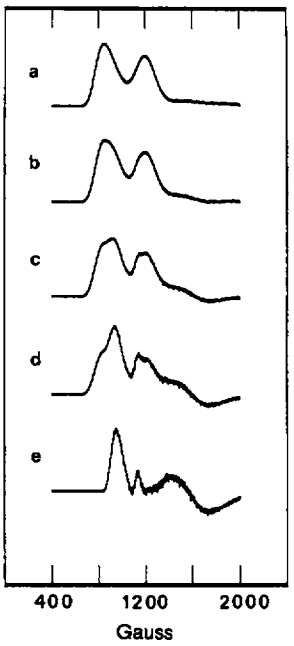

FIGURE 6 Different proportions of spectra with E/D = 0.06 or 0.10 are mixed to give the signals shown in this figure. The contributions from the lower and middle Kramers doublets are included. Additional simulation parameters are given in Table 1. The corresponding proportions of molecules that have E/D = 0.06 to those with E/D = 0.10 are (*a*) 0:1, (*b*) 1:99, (*c*) 1:35, (*d*) 1:15, and (*e*) 1:0. The appearance of "noise" in the simulated spectra is a manifestation of the angular mesh (1°) used in the calculation.

are compared with those used previously for $FeTfCO_3$ (16).

The g' values obtained from the EPR spectra of the other FeTfanion complexes were intermediate between those for $FeTfCO_3$ and FeTf malonate (Table 2) and are attributed to E/D ratios between ⅓ and 0.04. The combined data from the simulations and Table 2 show that the geometry of the iron site, as manifest in values of E/D, is sensitive to the donor strength of the proximal group on the anion. However, other features of the EPR spectra such as those arising from the conformational equilibrium that is influenced by chloride and the broad distributions of E/D values, are not correlated with the nature of the synergistic anion and may reflect features of protein structure in the vicinity of the metal-synergistic anion site.

ESEEM OF FeTfPYRUVATE

To determine whether the carboxylate group of the synergistic anion was bound to the iron in FeTfanion, ESEEM data were obtained for FeTfpyruvate and FeTf[1-^{13}C]pyruvate. The x-ray crystal structure of $FeTfCO_3$ showed a histidine coordinated to the iron at both of the metal-binding sites (11). ESEEM of $FeTfCO_3$ showed characteristic nitrogen frequencies of 0.70, 0.80, 1.57, and 2.3 MHz (9). Fourier transforms of the two-pulse and three-pulse ESEEM data for FeTfpyruvate (Fig. 9, *b* and *d*) included peaks at 0.78, 1.52, and 2.2 MHz due to the coordinated histidine nitrogen. The frequencies of these peaks are in good agreement with values observed previously for $FeTfCO_3$ (9), which indicates that the bonding to the coordinated nitrogen is relatively insensitive to the change in the synergistic anion. Comparison of the time-domain ESEEM data for FeTf pyruvate and FeTf[1-^{13}C]pyruvate (Fig. 10, *a* and *b*) clearly shows that the ^{13}C-nuclear spin has an impact on the modulation. The Fourier transform ESEEM data for

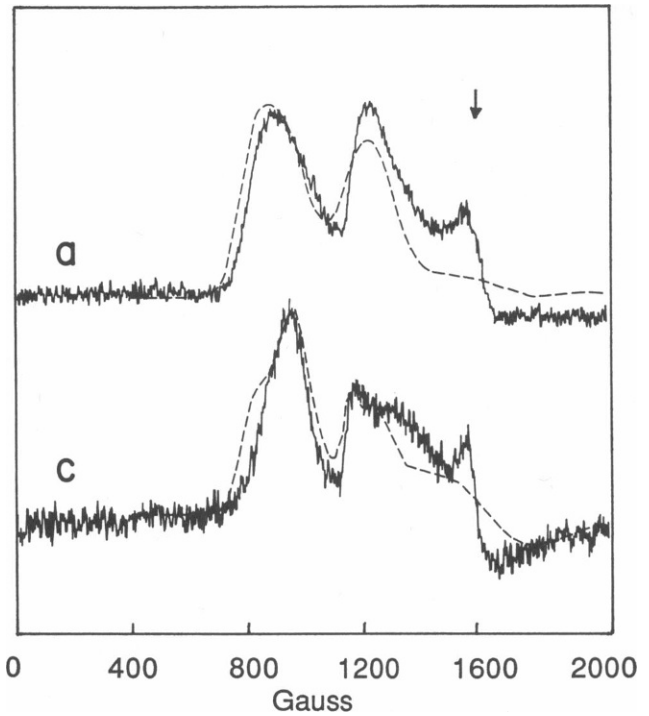

FIGURE 7 Spectra *b* and *d* from Fig. 6 are superimposed on the experimental spectra of Fig. 5, *a* and *c* for FeTfoxalate in 0 and 1.0 M NaCl. The contribution to the spectrum at $g' \sim 4.3$ from a small amount of $FeTfCO_3$ is marked with an arrow.

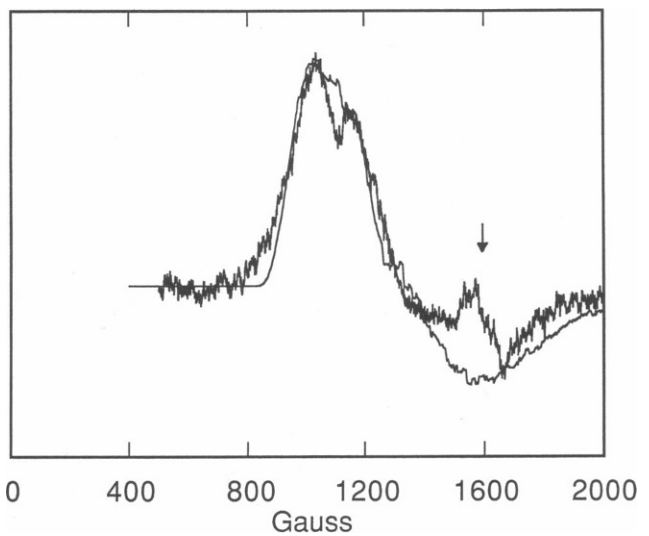

FIGURE 8 A simulation is compared with the experimental spectrum for FeTfmalonate. A single species was used in the simulation. Parameters for the simulation were *E/D*, 0.04; *D*, 0.25 cm^{-1}; width of *E/D* distribution, 0.02, and line width (FSL), 250 MHz. The contribution to the spectrum at $g' \sim 4.3$ from a small amount of $FeTfCO_3$ is marked with an arrow.

TABLE 1 **Simulation parameters for FeTfanion complexes**

Anion	*E/D*	*ΔE/D*	Linewidth*
Carbonate‡			*MHz*
Site 1	0.22	0.04	524
Site 2	0.325	0.12	313
Site 3	0.325 (minor)	none	§
Oxalate			
Site 1	0.06	0.015	150
Site 2	0.10	0.04	350
Malonate			
Site 1	0.04	0.02	250

*The lineshape is a frequency-swept Lorentzian with width = $\Delta\nu$. The apparent linewidth in Gauss is related to $\Delta\nu$ by: $\Delta\nu$ (in megahertz) × $0.714/g'$ = ΔB (Gauss) (reference 16).
‡Data reported in reference 16.
§See reference 16.

the [1-^{13}C]pyruvate complex show that the intensity at 3.0 MHz is increased in the two-pulse data (Fig. 9 *a*) and a new peak is present in the three-pulse data at 3.0 MHz (Fig. 9*c*) when compared with the data for FeTfpyruvate (Fig. 9, *b* and *d*). The two-pulse data also show a sum-peak at $\nu_C + \nu_H \simeq 9.8$ MHz (not shown). The frequencies of these peaks indicate an iron–^{13}C coupling constant of 1.3 MHz, which is similar to the value of 1.5 MHz that was observed for $FeTf^{13}CO_3$ (9). This coupling shows that the carbonate end of the pyruvate is bound to the iron.

TABLE 2 ***g'* Values from FeTfanion EPR spectra***

Anion	*g'*				
NTA	9.0	8.9		4.7 (sh)	~4.3‡
Glycolate	9.8	9.4		4.8 (sh)	~4.3
Lactate	9.7	9.0		4.8 (sh)	~4.3
Phenyllactate	9.7	9.0		4.9 (sh)	~4.3
Phenylalanine	9.7	9.0		5.0 (sh)	~4.3
Pyruvate	9.7	9.0		4.8 (sh)	~4.3
Carbonate	9.3	8.7		5.1 (sh)	~4.3
Glyoxalate	9.3	8.5 (br)		5.1 (sh)	~4.3
Salicylate	8.7			5.0	~4.3
Glycine	8.2 (br)			5.1	~4.3§
Maleate	8.1 (br)			5.0	~4.3
Oxalate			7.0 5.7	5.2	
Cyclohexyloxamate			7.0 5.9	5.2	
Malonate			6.6 5.9		
Group II anions that give composite spectra					
Malate			7.9 5.6	5.2 (sh)	~4.3
Aspartate	9.0		6.9	5.0	~4.3
Oxaloacetate	9.4	8.7	6.9	5.2	~4.3
α-Ketoglutarate			7.7 5.5		~4.3

**br* = broad, *sh* = shoulder.
‡Except for FeTfNTA, the $g' \sim 4.3$ peak was split.
§The $g' \sim 4.3$ peak has low intensity in this sample.

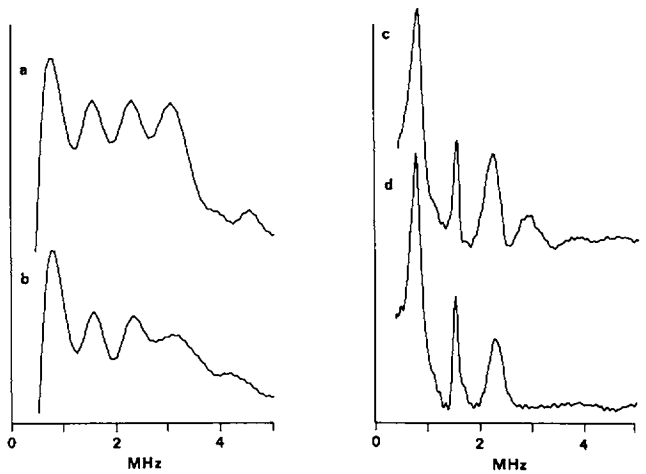

FIGURE 9 Cosine Fourier transform ESEEM data for FeTfpyruvate complexes. (*a*) Two-pulse data for FeTf[1-^{13}C]pyruvate. (*b*) Two-pulse data for FeTfpyruvate. (*c*) Three-pulse data for FeTf[1-^{13}C]pyruvate. (*d*) Three-pulse data for FeTfpyruvate.

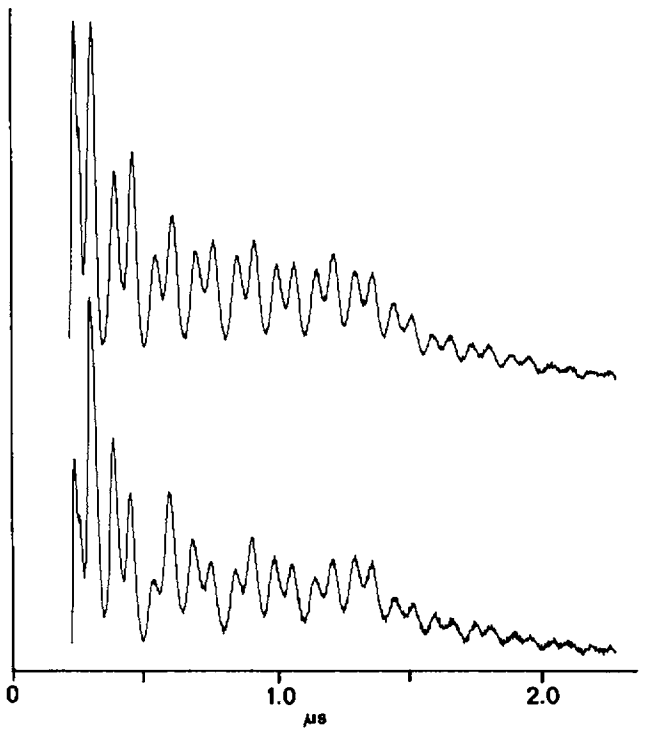

FIGURE 10 Two-pulse time-domain ESEEM data for (*a*) FeTfpyruvate and (*b*) FeTf[1-^{13}C]pyruvate. Data were obtained at 2–3 K and the magnetic field corresponding to the $g' = 4.3$ signal.

MODE OF ANION BINDING

Schlabach and Bates proposed (2) that the carbonate end of the synergistic anion was bound to the protein and only the proximal group was bound to the iron (see sketch in Fig. 11 *a*). Thus the ESEEM results require reconsideration of the mode of anion binding. An additional concern with the model proposed by Schlabach and Bates is that it requires a significantly different geometry of the anion binding site for these anions than for carbonate because the addition of a CHR group between the carboxylate and the group coordinated to the iron would require the iron and the anion binding site to be further apart than if carbonate were the anion.

The dependence of the EPR spectra for FeTfanion on the proximal group of the anion implies that the proximal group is bound to the iron. The ESEEM data for FeTf[1-^{13}C]pyruvate indicates that the carboxylate group is bound to the iron. Previously it had been shown that oxalate in CuTfoxalate and VOTfoxalate binds via both carboxylate groups (8). The combined information suggests that the synergistic anions bind as bidentate ligands with coordination of both the carboxylate and proximal groups. Several other pieces of information lend credence to this proposal. (*a*) In small-molecule chemistry, the anions in chart I are known to form unstrained bidentate complexes with bonding through the carboxylate and proximal groups. (*b*) The salicylate anion readily forms a chelate ring, but it would be difficult to distort it such that the hydroxy group is coordinated to the iron, and the carboxylate is not

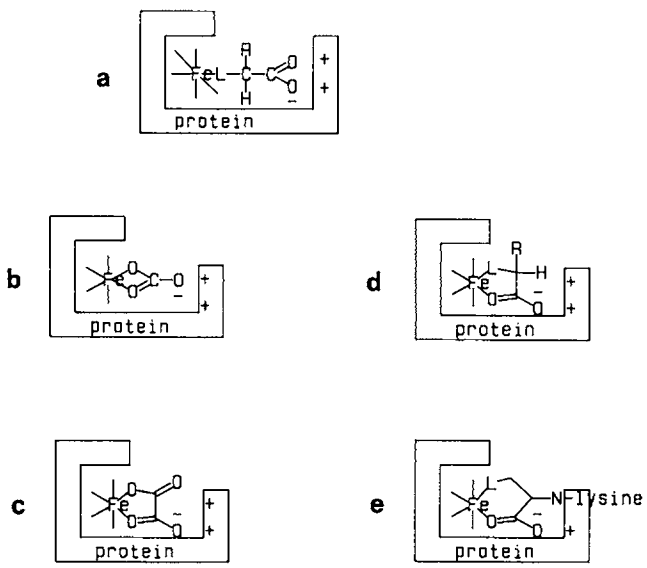

FIGURE 11 Schematic representations of binding modes for synergistic anions. (*a*) Model proposed by Schlabach and Bates, redrawn from Fig. 3 of reference 2. This model is not consistent with the ESEEM results obtained for FeTf[1-^{13}C]pyruvate. New models for bonding of carbonate (*b*), dicarboxylates (*c*), group I and II anions (*d*), and covalently attached anions (25) (*e*), based on the results of this study.

coordinated. (*c*) There are precedents in biological systems for bidentate coordination of anions in chart I via the carboxylate and proximal groups. EPR spectra indicated coordination of ^{17}O-labeled oxalate and glycolate to vanadyl pyruvate kinase through both the carboxylate and hydroxyl groups (23). ESEEM of [1-^{13}C]- and [2-^{13}C]-pyruvate demonstrated coordination of both the keto and carboxylate groups to vanadyl pyruvate kinase (24). NMR proton relaxivity studies of Co(II) carbonic anhydrase (25) and Cu(II) carbonic anhydrase (26) complexes with oxalate were interpreted in terms of coordination of both carboxylate groups. (*d*) After completion of this work, it was reported that the x-ray structure coordinates for $FeLfCO_3$ can accommodate coordination of oxalate via both carboxylate groups (13).

Fig. 11, *b–d* uses modifications of the diagram of Schlabach and Bates to illustrate the proposed model of bidentate anion coordination to the iron. Bidentate anion coordination is consistent with the CW EPR and ESEEM results and requires little change in the distance between the metal and the synergistic anion binding site while accommodating carbonate, dicarboxylate anions, and other difunctional anions.

It has been shown recently that bromopyruvate and hydroxypyruvate react with a lysine near the metal-binding site of the closely related protein ovotransferrin (27). These covalently bound groups are highly effective synergistic anions. It has been proposed that the ϵ-amino group of lysine is part of the anion binding site for transferrin (27), and the crystal structure of transferrin shows that there is a lysine in close proximity to the iron binding site (11). Coordination of the covalently attached anions can be accommodated in a diagram (Fig. 11 *e*) analogous to that proposed for the anions above.

CONCLUSIONS

The dependence of the EPR spectra of FeTfanion on the proximal group of the anion and the observation of Fe–^{13}C coupling in the ESEEM for FeTf[1-^{13}C]pyruvate indicate that both the carboxylate and proximal group are coordinated to the iron in FeTfanion complexes: the anions are bidentate. The variation in the proximal group of the anion causes the zero field splitting parameter ratio E/D to change from $\sim 1/3$ for carbonate to 0.04 for malonate. These observations lead to a new model for metal-site coordination of synergistic anions in transferrin: a carboxyl and one other polar group are ligands to the iron and the carboxyl also serves as a bridge between the iron and a positive charge on the protein. This bridge to the protein may be sensitive to factors including ionic strength and pH that influence release of iron from transferrin.

Support of this work by National Institutes of Health (NIH) grant GM21156 (G. R. Eaton and S. S. Eaton) and by NIH grant GM36232 (B. J. Gaffney) is gratefully acknowledged.

Received for publication 21 September 1990 and in final form 10 January 1991.

REFERENCES

1. Brock, J. 1985. Transferrins. *Topics Mol. Struct. Biol.* 7:183–262.
2. Schlabach, M. R., and G. W. Bates. 1975. The synergistic binding of anions and Fe^{3+} by transferrin. *J. Biol. Chem.* 250:2182–2188.
3. Folajtar, D. A., and N. D. Chasteen. 1982. Measurement of nonsynergistic anion binding to transferrin by EPR difference spectroscopy. *J. Am. Chem. Soc.* 104:5775–5780.
4. Kretchmar, S. A., and K. N. Raymond. 1988. Effects of ionic strength on iron removal from the monoferric transferrins. *Inorg. Chem.* 27:1436–1441.
5. Campbell, R. F., and N. D. Chasteen. 1977. An anion binding study of vanadyl (IV) human serotransferrin. *J. Biol. Chem.* 252:5996–6001.
6. Bertini, I., L. Messori, G. C. Pellacani, and M. Sola. 1988. Evidence of a metal-synergistic anion bond in thallium(III) transferrin. *Inorg. Chem.* 27:761–762.
7. Sola, M. 1990. ^{113}Cd and ^{13}C NMR of cadmium(II) transferrins. *Inorg. Chem.* 29:1113–1116.
8. Eaton, S. S., J. Dubach, K. M. More, G. R. Eaton, G. Thurman, and D. R. Ambruso. 1989. Comparison of the electron spin echo envelope modulation (ESEEM) for human lactoferrin and transferrin complexes of copper(II) and vanadyl ion. *J. Biol. Chem.* 264:4776–4781.
9. Eaton, S. S., J. Dubach, G. R. Eaton, G. Thurman, and D. R. Ambruso. 1990. Electron spin echo envelope modulation evidence for carbonate binding to iron(III) and copper(II) transferrin and lactoferrin. *J. Biol. Chem.* 265:7138–7141.
10. Bertini, I., C. Luchinat, L. Messori, A. Scozzafava, G. Pellacani, and M. Sola. 1986. ^{13}C NMR study of the synergistic anion in transferrins. *Inorg. Chem.* 25:1782–1786.
11. Bailey, S., R. W. Evans, R. C. Garratt, B. Gorinsky, S. Hasnain, C. Horsburgh, H. Jhoti, P. F. Lindley, A. Mydin, R. Sarra, and J. L. Watson. 1988. Molecular structure of serum transferrin at 3.3-A resolution. *Biochemistry.* 27:5804–5812.
12. Anderson, B. F., H. M. Baker, E. J. Dodson, G. E. Norris, S. V. Rumball, J. M. Waters, and E. N. Baker. 1987. Structure of human lactoferrin at 3.2-A resolution. *Proc. Natl. Acad. Sci. USA.* 84:1769–1773.
13. Baker, E. N., B. F. Anderson, H. M. Baker, M. Haridas, G. E. Norris, S. V. Rumball, and C. A Smith. 1990. Metal and anion binding sites in lactoferrin and related proteins. *Pure Appl. Chem.* 62:1067–1070.
14. Aisen, P., R. Aasa, B. G. Malmstrom, and T. Vanngard. 1967. Bicarbonate and the binding of iron to transferrin. *J. Biol. Chem.* 242:2484–2490.
15. Aisen, P., R. A. Pinkowitz, and A. Leibman. 1972. EPR and other studies of the anion-binding sites of transferrin. *Ann. NY Acad. Sci.* 222:337–346.

16. Yang, A.-S., and B. J. Gaffney, 1987. Determination of relative spin concentration in some high-spin ferric proteins using E/D-distribution in electron paramagnetic resonance simulations. *Biophys. J.* 51:55–67.

17. Najarian, R. C., D. C. Harris, and P. Aisen. 1979. Oxalate and spin-labeled oxalate as probes of the anion binding site of human transferrin. *J. Biol. Chem.* 253:38–42.

18. Bates, G. W., and J. Wernicke. 1971. The kinetics and mechanism of iron(III) exchange between chelates and transferrin. *J. Biol. Chem.* 246:3679–3685.

19. Bates, G. W., and M. R. Schlabach. 1975. The nonspecific binding of Fe^{3+} to transferrin in the absence of synergistic anions. *J. Biol. Chem.* 250:2177–2181.

20. Quine, R. W., G. R. Eaton, and S. S. Eaton. 1987. Pulsed EPR spectrometer. *Rev. Sci. Instrum.* 58:1709–1723.

21. Mims, W. B., 1984. Elimination of the dead-time artifact in electron spin-echo envelope spectra. *J. Magn. Reson.* 59:291–306.

22. Kretchmar, S. A., M. Teixeira, B.-H. Huynh, and K. N. Raymond. 1988. Mossbauer studies of electrophoretically purified monoferric and diferric human transferrin. *Biol. Metals* 1:26–32.

23. Lord, K. A., and G. H. Reed. 1984. Electron paramagnetic resonance studies of vanadyl complexes with pyruvate kinase. *Biochemistry.* 23:3349. (Abstr.)

24. Tipton, P. A., J. McCracken, J. B. Cornelius, and J. Peisach. 1989. Electron spin echo envelope modulation studies of pyruvate kinase active-site complexes. *Biochemistry.* 28:5720–5728.

25. Bertini, I., G. Canti, C. Luchinat, and A. Scozzafava. 1978. Characterization of cobalt(II) bovine carbonic anhydrase and of its derivatives. *J. Am. Chem. Soc.* 100:4873–4877.

26. Bertini, I., G. Canti, C. Luchinat, and A. Scozzafava. 1978. Spectroscopic investigation of copper(II) bovine carbonic anhydrase and its inhibitor derivatives. *J. C. S. Dalton.* 1269–1273.

27. Bailey, C. T., M. G. Patch, and C. J. Carrano. 1988. Affinity labels for the anion-binding site in ovotransferrin. *Biochemistry.* 27: 6276–6282.